Stability and Breakup of Thin Polar Films on Coated Substrates: Relationship to Macroscopic Parameters of Wetting

ARTICLE *in* INDUSTRIAL & ENGINEERING CHEMISTRY RESEARCH · SEPTEMBER 1996

Impact Factor: 2.59 · DOI: 10.1021/ie950775u

3 AUTHORS, INCLUDING:

Ahmad T. Jameel
International Islamic University Malaysia
21 PUBLICATIONS **125** CITATIONS
SEE PROFILE

Ashutosh Sharma IITK
Indian Institute of Technology Kanpur
336 PUBLICATIONS **7,416** CITATIONS
SEE PROFILE

Stability and Breakup of Thin Polar Films on Coated Substrates: Relationship to Macroscopic Parameters of Wetting

R. Khanna, A. T. Jameel,† and Ashutosh Sharma*

Department of Chemical Engineering, Indian Institute of Technology at Kanpur, Kanpur 208016, India

We study the linear and nonlinear stability, dynamics, and lifetimes of ultrathin (<100 nm) apolar and polar fluid films on uncoated and coated nonwettable substrates. The dynamics of nonequilibrium microscopic films is correlated to the equilibrium macroscopic parameters of wetting for coating and substrate. The equilibrium wettability (contact angle) of a coated substrate is determined almost entirely by coating properties. However, for films much thicker than the coating, the length scale of the instability is governed largely by the apolar surface properties of the substrate regardless of the apolar and polar properties of the coating. The film breakup time is more sensitive to the coating properties even for relatively thick films. The apolar and polar interactions with the coating control the instability of relatively thin films. For polar films, the actual (nonlinear) time of rupture may be several orders of magnitude smaller than the predictions of the linear theory.

Introduction

Stability, uniformity, and dewetting of ultrathin (<100 nm) films on nonwettable substrates are of technological and scientific interest in applications ranging from coatings, paints, adhesives, flotation, and lubrication to the fundamental understanding of multilayer adsorption,[29,47] wetting,[1−6,15,17,22,25,28,36,37,39,48] heterogeneous nucleation, cell adhesion,[9,12,13,27] near-interface diffusion,[31,33] morphology of nanostructures,[6,11,14,19,38,58] and tear film breakup.[42] In some applications (*e.g.*, thin film heat and mass-transfer devices), the initial film thickness may be beyond the range (∼100 nm) of the long-range intermolecular forces, but external disturbances, and other instabilities derived from evaporation, drainage, Marangoni flow, *etc.*, often decrease the film thickness locally so that the wetting properties assume significance in the formation of dry spots.[3,45] Bibliography given here is by no means exhaustive but illustrates a rich diversity of analyses and settings for thin films on solid substrates.

The free interface of an ultrathin film becomes unstable via a spinodal decomposition mechanism and deforms spontaneously whenever the intermolecular disjoining pressure increases with the film thickness; *i.e.*, the second derivative of the total excess free energy (per unit area) with respect to the film thickness is negative.[35,47,54] The initial growth of the interfacial instability eventually saturates when repulsive forces are present and become dominant.[19,38] A complex time-stationary structure consisting of an array of nanodrops in equilibrium with thin flat films finally emerges.[14,19,38,58] This phenomenon was termed as "morphological phase separation".[19,38] However, when the force field in the film is purely attractive, a true breakup (dewetting) of the film followed by the growth of circular dry patches on the substrate is the only possibility.[7,22,32,39,41,56,57] This is the case considered here.

The total surface tension, the interfacial tension, and the excess free energy of the film (compared to its bulk phase) are the sum of their respective apolar and polar components, which are engendered by the Lifshitz−van der Waals (LW) and the polar (P) interactions, respectively. The shorter ranged polar interactions, which are variously described as "acid−base" interactions,[50,51] hydrophobic interactions, hydration pressure, hydrogen bonding, *etc.*, also play an essential role in the determination of the substrate wettability (equilibrium contact angle)[1,17,21,23,37,49−53] and the film stability[19,36,38,39] in aqueous and polymeric systems. In fact, if only the apolar (LW) interactions are considered, thin aqueous films on most substrates (with surface tensions in excess of 21.8 mJ/m^2) should be stable and completely wetting.[36,38] In reality, most of these substrates are only partially wettable, and aqueous drops display finite contact angles due to a high polar component of the surface tension of water.[21,23,49−53]

While the ideal case of the instability of completely apolar films on pure and homogeneous substrates has been extensively studied,[7,15,22,27,28,35,43,44,47,54,56,57] real systems present many essential complexities which have to be considered. These include quantification of forces in the apolar and polar films on pure and coated substrates and the relationship between the film dynamics and the equilibrium substrate wettability. The first of these difficulties concerns the determination of the excess free energy (disjoining pressure) of the film. There is no simple way to directly measure or to predict the disjoining pressure for *nonequilibrium (unstable)* films, especially on variously modified, ill-defined substrates encountered in practice. For films on *uncoated* substrates, the strength of the polar and apolar interactions can, however, be related[36−39,50] to the apolar (S^{LW}) and polar (S^{P}) components of the total spreading coefficient, S, defined as

$$S = \gamma_{sb} - \gamma_{sf} - \gamma_{fb} = S^{LW} + S^{P} \qquad (1)$$

where γ_{ij} is the total interfacial tension between i and j, which is the sum of its apolar (γ_{ij}^{LW}) and polar (γ_{ij}^{P}) components.[50,51] Subscripts identify the following phases: s is substrate, b is bounding fluid, and f is film fluid (Figure 1). Further, the equilibrium contact angle, θ, (wettability) of a macroscopic drop of the film fluid

* Corresponding author. Fax: 91-512-250007 or 250260. Telephone: 91-512-257026. Email: ashutos@iitk.ernet.in.

† Present address: Department of Chemical Engineering, Aligarh Muslim University, Aligarh 202002, India.

S0888-5885(95)00775-5 CCC: $12.00

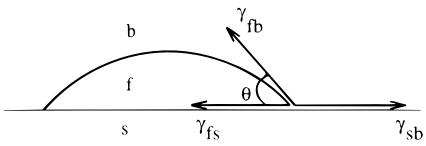

Figure 1. Equilibrium contact angle of a large drop of fluid (f) on substrate (s) in the presence of bounding fluid (b) is given by the horizontal resolution of interfacial tensions at the three-phase contact line.

in the presence of bounding fluid is also related to S by the Young−Dupré equation (Figure 1).

$$\gamma_{fb} \cos\theta + \gamma_{sf} = \gamma_{sb} \quad \text{or} \quad 1 + \cos\theta = S/\gamma_{fb} \qquad (2)$$

The Young−Dupré equation (2) without the film pressure also results[37] directly from the modified Young−Laplace equation of capillarity for the case considered here (S^{LW}, $S^{P} \leq 0$). Clearly, a negative spreading coefficient implies partial wetting, which also results in greater destabilization of the thin film.[36,38,39]

While measurements of S^{LW} are more facile,[36,50,51] evaluation of S^{P} usually involves estimations of the acid−base or polar parameters of the liquid and the substrates.[21,23,36,38,49−53] We present a parameterless method for determination of S^{LW} and S^{P} and the excess free energy from contact angle measurements.

The first objective of this paper is to explore relationships between thin film stability (and dynamics) and the equilibrium macroscopic parameters of wetting (S^{LW}, S^{P}, and θ), *when both the components of the spreading coefficient are negative* (S^{LW}, $S^{P} < 0$), *i.e., when both the long- and short-range interactions are destablizing (attractive).* As is shown later, water films (bounded by gas) on low-energy substrates (*e.g.*, Teflon) satisfy these conditions. Water films, bounded by apolar hydrocarbon phases, on high-energy substrates also display S^{LW}, $S^{P} < 0$. For such cases, both the apolar (long-range) and polar (short-range) forces promote dewetting, as shown in a short note earlier.[39]

The second difficulty concerns the effect of thin surface coatings of the substrate on the film stability. Some fascinating aspects of wetting of coated (stratified) substrates by drops have been studied previously.[2] It has been demonstrated that nanosized coatings can alter the equilibrium contact angle (wettability) of a substrate rather profoundly.[10,24,32,59] However, the influence of coating properties on the film stability has not been studied, except in a recent simplified analysis.[41] This aspect is important because, in most applications (*e.g.*, biomaterials, flotation), the substrate properties and wettability are tailored by application of thin coatings by different techniques, *e.g.*, Langmuir−Blodgett deposition, self-assembled monolayers, polymer brushes, *etc.*[55] Even in the absence of deliberately applied coatings, few substrates can be considered homogeneous right up to their surfaces. Surface contamination, adsorption from solutions and polymer melts, hydration, and reactions (*e.g.*, Si → SiO_2) also engender pseudocoatings of vastly different surface properties and wettability.

The second objective of this paper is to study the effect of surface coatings on the film stability and dynamics and to correlate the stability with the spreading coefficients of the substrate and the coating materials. *In particular, we consider the process of film breakup when coating as well as the underlying substrate is nonwettable, and a true dewetting occurs.* True dewetting by the spinodal decomposition mechanism can occur only when both the long-range and the short-range interactions of the film with the coating and substrate are purely attractive (destabilizing).[36−39] In other cases, a short-range repulsion usually stabilizes the film against rupture and the film merely becomes rough.[19,36,38]

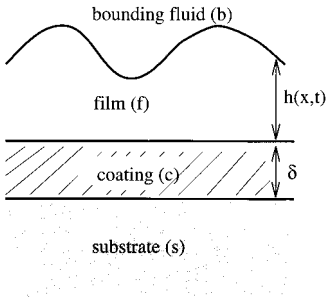

Figure 2. Schematic of an unstable thin film on coated substrate.

To summarize, we explore the linear and nonlinear stability, dynamics, and breakup of ultrathin films on pure and coated nonwettable substrates and correlate the film dynamics to the equilibrium macroscopic parameters of wetting (spreading coefficient, contact angle). In contrast to the difficulties in determination of the excess free energy of the film due to intermolecular interactions, the equilibrium macroscopic parameters of wetting are easily quantified by facile measurements of equilibrium contact angle of large drops.

Thin Film Equation

We consider the instability and breakup of an ultrathin (<100 nm) liquid film on a nonwettable coated substrate (Figure 2). Two-dimensional fluid flow in the film is governed by the Navier−Stokes equations with the inclusion of excess body forces derived from the intermolecular interactions, which depend on the local film thickness. The instability (deformation) of the free surface evolves on a length scale (wavelength) which is large compared to the film thickness. This allows considerable simplification of the equations of motion and associated boundary conditions at the free interface in the "lubrication" approximation, or the "long-wave" approximation.[35,56] The following equation describes the shape and dynamics of a thin film sandwiched between an inviscid fluid and a solid:[9,38,43,56]

$$3\mu \frac{\partial h}{\partial t} + \frac{\partial}{\partial x}\left(\gamma_{fb} h^3 \frac{\partial^3 h}{\partial x^3}\right) - \frac{\partial}{\partial x}\left[h^3\left(\frac{\partial^2 \Delta G}{\partial h^2}\right)\frac{\partial h}{\partial x}\right] = 0 \qquad (3)$$

where $h(x,t)$ is the local film thickness, coordinate x runs parallel to the substrate surface, t is time, μ is viscosity, γ_{fb} is interfacial tension of the film (f) against the bounding phase (b), and ΔG is the total excess free energy per unit area of the film due to various intermolecular interactions. Viscous effects in the bounding medium can be neglected when its viscosity is comparable to the film viscosity.[27] For films rendered tangentially immobile by the presence of surfactants, the viscous coefficient 3 is replaced by 12.[43] Equation 3 may be viewed simply as the sum of the three forces (from left to right): viscous force, interfacial force due to curvature of the free interface, and the excess intermolecular force. The viscous force *retards* the growth of instability, whereas the interfacial tension has a *stabilizing* influence until the film ruptures. The last term has the form of a diffusion operator (in h) with variable

diffusivity, $h^3(\partial^2\Delta G/\partial h^2)$. Thus, negative diffusivity ($\partial^2\Delta G/\partial h^2 < 0$) leads to the interfacial instability manifested as the growth of the thicker regions at the expense of thinner regions of the film. The condition $\partial^2\Delta G/\partial h^2 < 0$ is, of course, common to all sorts of spinodal decomposition processes. A true breakup of the film and formation of dry spots, however, occur only when the condition $\partial^2\Delta G/\partial h^2 < 0$ is satisfied for *all* film thicknesses ($h > 0$).

Finally, the disjoining pressure[8] of a thin film (compared to bulk) is defined as $\Pi = -\partial\Delta G/\partial h$, and the excess potential (per unit volume) of the film molecules at the free interface is $\phi = -\Pi$.

Excess Free Energy of Film

In the absence of significant electrical double layer effects, the total excess free energy is derived from the long-range apolar Lifshitz−van der Waals (LW) interactions and from the shorter-ranged polar (*e.g.*, acid−base) interactions, which become significant for hydrogen-bonding substances like aqueous systems.

The LW component of the excess interaction potential (per unit volume), ϕ^{LW}, is made up of six different LW interactions: (1) interactions among the molecules of the film of thickness h, (2) interactions among the molecules of the film and the coating of thickness δ, (3) interactions among the molecules of the film and the bulk substrate, (4) interactions among the molecules of the film and overlying bulk bounding fluid, (5) interactions among the molecules of the bounding medium and coating, and finally (6) interactions among the molecules of the bounding medium and the substrate.

The total excess LW potential, $\phi^{LW} = \partial\Delta G^{LW}/\partial h$, is readily evaluated by pairwise summation of intermolecular LW potentials (with r^{-6} decay) in the microscopic approach of London and Hamaker (see, *e.g.*, refs 16 and 29).

$$\phi^{LW} = \frac{1}{6\pi h^3}(A_{ff} + A_{cb} - A_{fb} - A_{cf}) + \frac{1}{6\pi(h+\delta)^3}(A_{cf} + A_{sb} - A_{cb} - A_{sf}) \quad (4)$$

where A_{ij} refers to the Hamaker constant (in J) for LW interactions between molecules of type i and j, and subscripts f, c, s, and b denote the film, coating, substrate, and bounding fluid materials, respectively.

As expected, the excess potential vanishes for a thick film ($h \to \infty$) and reduces to the well-known form $A_e/6\pi h^3$ in the limits of $\delta \to 0$ (absence of coating) and $\delta \to \infty$ (thick coating).

For $\delta \to 0$, the effective Hamaker constant in eq 4 is for the pure (uncoated) substrate, *viz.*, $A_e = A_{ff} + A_{sb} - A_{sf} - A_{fb}$.[36,42] For $\delta \to \infty$, or $\delta \gg h$, the effect of the substrate is screened out, and the effective Hamaker constant, A_e, is, as expected, given by $A_{ff} + A_{cb} - A_{cf} - A_{fb}$. Further, when the bounding fluid is a gas, $A_{cb} = A_{sb} = A_{fb} = 0$, only three Hamaker constants, A_{ff}, A_{cf}, and A_{sf} are sufficient to specify the excess potential of the film.[2,41]

Relationship of Excess Free Energy to Spreading Coefficients

The LW component of the excess free energy per unit area is obtained from eq 4 by noting that $\Delta G = \int \phi^{LW}\, dh$

$$\Delta G^{LW} = -\frac{A_{e1}}{12\pi h^2} - \frac{A_{e2}}{12\pi(h+\delta)^2} \quad (5)$$

where $A_{e1} = A_{ff} + A_{cb} - A_{fb} - A_{cf}$ and $A_{e2} = A_{cf} + A_{sb} - A_{cb} - A_{sf}$.

As is well-known,[18,50,51] a complete disappearence of the film does not correspond to $h \to 0$, where expression (5) diverges, but to $h \to d_0$, where d_0 is a "cut-off" equilibrium distance where the extremely short-range Born repulsion (due to r^{-12} term in Lennard-Jones potential) may be replaced by a vertical rise in the potential to infinity (hard-sphere approximation). The best value for d_0 is found to be 0.158 ± 0.008 nm for a vast array of materials.[50,51]

While the Hamaker constants cannot be evaluated in the absence of detailed spectroscopic data, they can be related to the LW component of the spreading coefficient by performing a simple thought experiment. Consider an initially thick film ($h \to \infty$) which is made to disappear ($h \to d_0$) on a thick coating ($\delta \to \infty$). The change in the LW component of the free energy (per unit area) in this process is given by

$$\Delta G^{LW} = \gamma_{cb}^{LW} - (\gamma_{fb}^{LW} + \gamma_{cf}^{LW}) \quad (6)$$

The same change in energy from eq 5 is $-A_{e1}/12\pi d_0^2$. Equating the two expressions for ΔG^{LW} gives[36,51]

$$A_{e1} = -12\pi d_0^2(\gamma_{cb}^{LW} - \gamma_{fb}^{LW} - \gamma_{cf}^{LW}) = -12\pi d_0^2 S_c^{LW} \quad (7)$$

where S_c^{LW} is the LW component of the spreading coefficient of the film fluid (f) on bulk coating material (c) in the presence of the bounding phase (b).

Similarly, on an *uncoated substrate* ($\delta \to 0$), the change in the LW component of the free energy in reducing the film thickness from $h \to \infty$ to $h = d_0$ is $[\gamma_{sb}^{LW} - (\gamma_{fb}^{LW} + \gamma_{sf}^{LW}]] = S_s^{LW}$, which also equals $[-(A_{e1} + A_{e2})/12\pi d_0^2]$ from eq 5. This procedure, with the help of eq 7, gives

$$A_{e2} = -12\pi d_0^2(S_s^{LW} - S_c^{LW}) \quad (8)$$

where S_s^{LW} is the LW component of the spreading coefficient.

The LW components of the spreading coefficients can also be defined in terms of the LW components of the surface tensions (against air), γ_i, by the use of Good−Girifalco−Fowkes combining rule (see, *e.g.*, refs 50 and 51),

$$\gamma_{ij}^{LW} = [\sqrt{\gamma_i^{LW}} - \sqrt{\gamma_j^{LW}}]^2 \quad (9)$$

thus

$$S_k^{LW} = 2[\sqrt{\gamma_k^{LW}} - \sqrt{\gamma_f^{LW}}][\sqrt{\gamma_f^{LW}} - \sqrt{\gamma_b^{LW}}] \quad (10)$$

where k may refer either to substrate (s) or to coating (c). With the help of eq 10, it can be verified that expressions (7) and (8) can also be obtained formally by noting that $A_{ij} = \sqrt{A_{ii}A_{jj}}$ and $A_{ii} = 24\pi d_0^2\gamma_i^{LW}$.[36,51]

The shorter-ranged polar component of the excess free energy is due to the various combinations of the polar interactions among molecules of the film, bounding fluid, and the top layer of the surface molecules.[36−38,50,51]

$$\Delta G^{\mathrm{P}} = S_k^{\mathrm{P}} \exp[(d_0 - h)/l_0] \qquad (11)$$

where l_0 is a correlation length for the decay of polar interactions in the film (0.2−1 nm for water),[50,51] and S_k^{P} is the polar component of the spreading coefficient on the top layer of the surface (subscript k refers either to coating or to substrate for coated and uncoated substrates, respectively), S_k^{P} is defined in terms of the polar components of the interfacial tensions, γ_{ij}^{P}, as

$$S_k^{\mathrm{P}} = \gamma_{k\mathrm{b}}^{\mathrm{P}} - \gamma_{k\mathrm{f}}^{\mathrm{P}} - \gamma_{\mathrm{fb}}^{\mathrm{P}}; \qquad k = \mathrm{s, c} \qquad (12)$$

Clearly, S_k^{P} is also the change in the polar component of the free energy during the disappearence ($h \rightarrow d_0$) of an initially macroscopic ($h \rightarrow \infty$) film.[36] The polar component of the interfacial tension, γ_{ij}^{P}, can be simplified in the following cases:[51]

$$\gamma_{ij}^{\mathrm{P}} = \begin{cases} \gamma_i^{\mathrm{P}} & \text{if } j \text{ is apolar} \\ 0 & \text{if } i \text{ and } j \text{ are both apolar} \end{cases} \qquad (13)$$

With the help of eqs 5, 7, 8, and 11, the total excess free energy is given by

$$\Delta G = S_{\mathrm{c}}^{\mathrm{LW}} \frac{{d_0}^2}{h^2} + (S_{\mathrm{s}}^{\mathrm{LW}} - S_{\mathrm{c}}^{\mathrm{LW}}) \frac{{d_0}^2}{(h+\delta)^2} + S_k^{\mathrm{P}} \exp[(d_0 - h)/l_0] \qquad (14)$$

In eq 14, the LW interaction with the substrate is the long-range component, since for sufficiently thick films ($h \gg \delta$), $\Delta G \propto S_{\mathrm{s}}^{\mathrm{LW}}$, regardless of coating properties. The LW and the polar interactions with the coating are both short-ranged, the latter because of their exponential decay and the former because for sufficiently thin films ($h \ll \delta$), $\Delta G \propto S_{\mathrm{c}}^{\mathrm{LW}}$, regardless of the substrate properties. In more complex systems (*e.g.*, polymer films on grafted polymer "brushes"[34]), other short-range entropy-driven interactions leading to "autophobic" behavior are also possible.[26,46] Regardless of the physical origin of the interactions, eq 14 provides a convenient prototype for the study of rupture of films subjected to long- and short-range attractive interactions.

Determination of Apolar and Polar Components of the Spreading Coefficient

Based on rule (13) and eq 12, it is easily verified that the system consisting of the surface (k)−film (f)−bounding fluid (b) is completely apolar ($S_k^{\mathrm{P}} = 0$) only when the film fluid *and* at least one of the bounding phases (k or b) are apolar (*e.g.*, gases, hydrocarbons). For aqueous films, however, S^{P} is almost always negative due to a large polar component of the cohesive energy of water ($\gamma_{\mathrm{w}}^{\mathrm{P}} = 51$, $\gamma_{\mathrm{w}}^{\mathrm{LW}} = 21.8$; in mJ/m^2). The minimum value of $S^{\mathrm{P}} = -2\gamma_{\mathrm{w}}^{\mathrm{P}} = -102$ mJ/m^2 is obtained for water when the surface and the bounding fluid are both apolar. An increased polarity of the surface, however, makes S^{P} less negative.

Table 1. Apolar and Polar Components of the Spreading Coefficient of Water

substrate−water−bounding fluid	S^{LW} (mJ/m^2)	S^{P} (mJ/m^2)	ref[a]
Teflon−air	−5.1	−102	53
apolar surface−octane	0	−102	*b*
poly(hexafluoropropylene)−air	−11.7	−90	21
perfluorolauric acid−air	−16.5	−76.5	21
ω-monohydro−air	−7.0	−75.7	21
60 TFE-40 Kel-F copolymer−air	−1.1	−77.0	21
human fibrinogen (dry)−*n*-hexadecane[c]	−1.8	−23.8	49
human fibrinectin (dry)−*n*-hexadecane[c]	−0.8	−8.7	49
cellulose acetate−carbon tetrachloride[d]	−1.5	−22.6	52

[a] References from which values of γ_i^{LW} for the substrate and equilibrium contact angles of water are taken for computations of S^{LW} and S^{P}. [b] γ^{LW}(octane) ≃ γ^{LW}(water) = 21.8 mJ/m^2. [c] γ^{LW}(*n*-hexadecane) = γ = 27.1 mJ/m^2.[49] [d] γ^{LW}(carbon tetrachloride) = 26.8 mJ/m^2.[52]

Based on eq 10, apolar (LW) forces also encourage dewetting ($S_k^{\mathrm{P}} < 0$) whenever one of the following two conditions are met:

$$\gamma_k^{\mathrm{LW}}, \gamma_{\mathrm{b}}^{\mathrm{LW}} > \gamma_{\mathrm{f}}^{\mathrm{LW}}$$

$$\gamma_k^{\mathrm{LW}}, \gamma_{\mathrm{b}}^{\mathrm{LW}} < \gamma_{\mathrm{f}}^{\mathrm{LW}} \qquad (15)$$

Thus, S^{LW} is negative for water films (bounded by gas or low surface tension hydrocarbons) on low-energy surfaces ($\gamma_k^{\mathrm{LW}} < 21.8$ mJ/m^2) as well as for water films sandwiched between higher surface energy media γ_k^{LW}, $\gamma_{\mathrm{b}}^{\mathrm{LW}} > 21.8$ mJ/m^2. When S^{LW} and S^{P} are both negative, their magnitudes can be obtained by the methodology given in the appendix, without resorting to the models of polar or acid−base interactions.[50,51] Some representative values of S^{LW} and S^{P} thus estimated based on the contact angle data available elsewhere are summarized in Table 1.

The maximum negative values of S^{LW} are obtained for water films bounded by air on low-energy surfaces (*e.g.*, HEMA/EMA grafted polyethylene with γ^{LW} as low as 4.4 mJ/m^2).[23] S^{LW} for water films bounded by hydrocarbons on most polymeric and biological surfaces is small. However, water on metal surfaces ($\gamma^{\mathrm{LW}} \sim$ 100−1000 mJ/m^2) when bounded by hexadecane can have more negative S^{LW} in the range of −5 to −27 mJ/m^2.

An interesting example is that of water drop/film bounded by octane[20,23] for which $S^{\mathrm{LW}} \simeq 0$ due to $\gamma_{\mathrm{f}}^{\mathrm{LW}} \simeq \gamma_{\mathrm{b}}^{\mathrm{LW}} \simeq 21.8$ mJ/m^2 regardless of the nature of the surface. A neglect of the polar "hydrophobic" interactions would lead to (incorrect) conclusions that equilibrium contact angle is zero, water drops should completely spread out, and thin films of water (when surrounded by octane) are unconditionally stable. In reality, surface−water−octane systems display large contact angles approaching 180° on the apolar surfaces[20] since $S^{\mathrm{P}} = -102$ mJ/m^2. A large polar component of the free energy signifies a strong tendency of such films to rupture and recede from the surface. This and other examples of Table 1 emphasize that the LW interactions alone cannot explain the wetting behavior of thin films of water (and other polar liquids) even qualitatively.

Evaluation of the free energy on coated substrates (eq 14) requires estimation of S^{LW} for the coating as well as the substrate materials. In some of the most popular methods of coating (*e.g.*, Langmuir−Blodgett, self-assembled monolayers), a large amount of coating material in its bulk form is not available to carry out

the contact angle measurements as outlined in the appendix. Further, the polar interactions are very sensitive to the structure of the top layers of the molecules of the coating, which may depend on the substrate properties and the coating thickness. It is therefore desirable to determine S_c^{LW} and S_c^{P} for the coating by measurements of the contact angle on the *coated substrate* directly. The equilibrium contact angle of liquid (f) in the presence of a bounding medium (b) on the coated substrate can be obtained from the modified Young−Dupré equation[1,2,17,37]

$$\cos\theta = 1 + \frac{\Delta G_m}{\gamma_{fb}} \tag{16}$$

where ΔG_m is the minimum value of the free energy. When both the apolar and polar forces promote dewetting, *i.e.*, S_s^{LW}, S_c^{LW}, and $S_c^{P} < 0$, the free-energy minimum occurs at the cut-off distance, $h = d_0$,[37] due to the Born repulsion (see eq 14). Evaluating ΔG at d_0 from eq 14 and combining with eq 16 give the contact angle on coated substrate.

$$\cos\theta_c = 1 + \frac{1}{\gamma_{fb}}\left[S_c^{LW} + S_c^{P} + \frac{{d_0}^2}{(d_0+\delta)^2}(S_s^{LW} - S_c^{LW})\right] \tag{17}$$

It reduces to the Young−Dupré equation (2) for uncoated substrate ($\delta \to 0$). In general, θ_c depends on properties of both the coating (S_c^{LW}, S_c^{P}, and δ) and the substrate (S_s^{LW}). However, most coatings, including monolayers of organic films, are at least about a nanometer thick, so that $d_0^2/(d_0+\delta)^2$ can be neglected in eq 17 since $d_0 \sim 0.158$ nm. Thus, contact angle measurements on coated substrates essentially yield information only on coating properties as the long-range (LW) interactions with the substrate are almost completely screened near the three-phase contact line (see predictions of eq 14 as $h \to d_0$). The conclusion that the equilibrium wetting behavior of coated substrates is determined almost entirely by the coating properties is also experimentally well supported.[10,24,32,59] Interestingly, as is shown in the next section, the length and time scales of instability of relatively thick films ($h \gg \delta$) are governed largely by the substrate properties, regardless of the properties of the coating. However, the length scale is much less sensitive to the coating properties compared to the breakup time.

Film Stability and Dynamics

The thin film equation (3) combined with the expression for the free energy (14) can be represented in a compact form with the help of the following nondimensional quantities ($S^{LW} < 0$, $S^{P} \le 0$):

$$H = h/h_0, \quad d = d_0/h_0, \quad l = l_0/h_0, \quad C = 3\rho\nu^2/\gamma_{fb}h_0 \tag{18a}$$

$$B = -6S_s^{LW}h_0d^2/3\rho\nu^2, \quad P = (S_k^{P}/S_s^{LW})(1/6d^2l^2) \tag{18b}$$

$$R = S_c^{LW}/S_s^{LW}, \quad D = \delta/h_0 \tag{18c}$$

and nondimensional space and time scalings

$$X = x/x_c, \quad T = t/t_c, \quad x_c = h_0(|B|C)^{-1/2}, \quad t_c = (h_0^2/\nu)(B^2C)^{-1} \tag{19}$$

where h_0 is the mean film thickness, ρ is density of the film fluid, and ν is kinematic viscosity, μ/ρ.

As is shown later based on the nonlinear stability analysis (eqs 27 and 28), x_c and t_c are proper characteristic length and time scales for instability engendered by the LW forces. This is the reason why scalings (19) lead to the most compact nondimensional representation of the results. The nondimensional evolution equation for the film thickness in the strongly conservative form is

$$\frac{\partial H}{\partial T} + \frac{\partial}{\partial X}\left[H^3\frac{\partial}{\partial X}\left[\frac{\partial^2 H}{\partial X^2} - \frac{1}{3H^3}\left\{\left(1+\frac{D}{H}\right)^{-3}(1-R) + R\right\} - Pl\exp\left\{\frac{d-H}{l}\right\}\right]\right] = 0 \tag{20}$$

The second and fourth terms in eq 20 describe the stabilizing effects of the apolar and polar forces, respectively. The case of pure uncoated substrate is recovered[38] for $R = 1$ (and also for $R = 0$, $D = 0$). The case of a thick coating corresponds to $D \to \infty$. The completely apolar case corresponds to $P = 0$. However, scalings (18b) and (19) are not suitable for the completely polar case ($\gamma_f^{LW} = \gamma_b^{LW}$, $S^{LW} = 0$) discussed earlier (surface−water−octane system), for which $P \to \infty$. For this case, it is best to render eq 3 nondimensional with the help of scalings (18a) and the following transformations:

$$F = -S^{P}h_0/3\rho\nu^2, \quad X^* = (FC)^{1/2}, \quad T^* = (F^2C)(\nu/h_0^2)t \tag{21}$$

The nondimensional equation of evolution for completely polar films $S_c^{LW} = S_s^{LW} = 0$ and $S_k^{P} \neq 0$ is

$$\frac{\partial H}{\partial T^*} + \frac{\partial}{\partial X^*}\left[H^3\frac{\partial^3 H}{\partial X^{*3}} + \frac{H^3}{l^2}\exp\left\{\frac{d-H}{l}\right\}\frac{\partial H}{\partial X^*}\right] \tag{22}$$

Linear Stability Analysis. The initial (short-time) evolution of infinitesimal disturbances is obtained by linearization of eq 20 around the mean film thickness ($H = 1$), which gives

$$H = 1 + \epsilon\exp(\iota KX + \omega T) \tag{23}$$

The nondimensional growth coefficient, ω, depends on the nondimensional wavenumber, K.

$$\omega = K^2\left[\{(1+D)^{-4}(1-R) + R\} + P\exp\left\{\frac{d-1}{l}\right\}\right] - K^4 \tag{24}$$

The film is linearly unstable ($\omega > 0$) to a range of wavenumbers, $K < K_C$, where $\omega(K_C) = 0$. The most unstable (fastest-growing) mode of the linear theory evolves on a length scale, $\Lambda_{ML} = 2\pi/K_{ML}$ which satisfies $\partial\omega/\partial K = 0$, *viz.*, $K_{ML} = K_C/\sqrt{2}$.

$$\Lambda_{ML} = 2\sqrt{2}\pi\left[\{(1+D)^{-4}(1-R) + R\} + P\exp\left\{\frac{d-1}{l}\right\}\right]^{-1/2} \tag{25}$$

An estimate for the minimum time of film rupture may

be obtained from the linear theory by setting $H = 0$ and $\omega = \omega(K_{ML})$.

$$T_{ML} = 4\left[(1 + D)^{-4}(1 - R) + R + P \exp\left\{\frac{d-1}{l}\right\}\right]^{-2} \ln\left(\frac{1}{\epsilon}\right) \quad (26)$$

The time of rupture from the linear theory for $K \neq K_{ML}$ is also easily obtained from the definition $T_L(K) = \ln(1/\epsilon)/\omega(K)$. While the nondimensional version, eq 20, is extremely economical for numerical solutions, the physics can be better appreciated with the help of dimensional counterparts to eqs 25 and 26, which are

$$\lambda_{ML}^2 = -4\left(\frac{4\pi^2\gamma_{fb}h_0^4}{3d_0^2 S_s^{LW}}\right)\left[(1 + D)^{-4}(1 - R) + R + \left(\frac{h_0^2}{d_0 l_0}\right)^2\left(\frac{S_k^P}{6S_s^{LW}}\right)\exp\left\{\frac{d_0 - h_0}{l_0}\right\}\right]^{-1} \quad (27)$$

$$t_{ML} = \left[\frac{\mu\gamma_{fb}h_0^5}{3(S_s^{LW})^2 d_0^4}\right]\left[(1 + D)^{-4}(1 - R) + R + \left(\frac{h_0^2}{d_0 l_0}\right)^2\left(\frac{S_k^P}{6S_s^{LW}}\right)\exp\left\{\frac{d_0 - h_0}{l_0}\right\}\right]^{-2} \ln\left(\frac{1}{\epsilon}\right) \quad (28)$$

Clearly, decreased wettabilities of the coating and substrate (more negative S_c^{LW}, S_s^{LW}, and S_k^P) engender faster rupture by shorter waves. The latter indicates an increased density of holes in the film.

Similarly, for completely polar films (surface−water−octane system), eq 22 gives the growth coefficient, wavelength of the dominant mode, and the time of rupture, respectively, as expressions

$$\omega^* = \left(\frac{K^*}{l}\right)^2 \exp\left\{\frac{d-1}{l}\right\} - K^{*4} \quad (29)$$

$$\Lambda_{ML}^* = \sqrt{2}\Lambda_C^* = 2\sqrt{2}\pi l \exp\left\{\frac{d-1}{2l}\right\} \quad (30)$$

$$T_{ML}^* = 4l^4 \exp\left\{\frac{2(d-1)}{l}\right\} \ln\left(\frac{1}{\epsilon}\right) \quad (31)$$

Equations 24−31 relate the thin film stability and dynamics to equilibrium macroscopic parameters of wetting—S_s^{LW}, S_c^{LW}, and S_k^P, all of which may be determined by equilibrium contact angle measurements as shown in the appendix. These relations are, however, valid only in the linear regime.

Numerical Method. Nonlinear equations (20) and (22) were also solved numerically in order to assess the role of nonlinear interactions in the growth of instability. The lateral dimensions of the film are considered to be much larger than the length scale of the instability, which rarely exceeds 100 μm. Thus, periodic boundary conditions are more meaningful for the study of instability on its natural length scale, when the end effects (on the film scale) are not considered. A pseudo spectral method−Fourier collocation was used for numerical simulations satisfying periodic boundary conditions over a wavelength $X \in (0, \Lambda)$ and an initial condition $H(0,X) = 1 + \epsilon \sin KX$. In a few simulations, volume-preserving random initial conditions with a specified maximum amplitude were used. The dominant wavelength of linear theory, Λ_{ML}, was used in simulations, except when the influence of domain size Λ was studied. Values of d_0 and l_0 were chosen to be 0.158 and 0.6 nm, respectively,[50,51] in simulations reported here. Forty to sixty-four spatial collocation points were found satisfactory, and the resulting set of equations were integrated in time by a GEAR algorithm for stiff equations. Further details of the method and its applications to thin films may be found elsewhere.[38,40]

Results and Discussion

Since the polar interactions depend crucially on the surface properties of the top layer of the surface molecules, the most profound influence of the coating is to change the polar component of the spreading coefficient S_k^P from S_s^P (for uncoated substrate) to S_c^P (for coating). The long-range LW interactions are also modified. *In the linear approximation*, eqs 25−28 suggest that for a *coated substrate* an effective LW component of the spreading coefficient may be defined as

$$S_e^{LW} = S_s^{LW}[(1 + D)^{-4}(1 - R) + R] \quad (32)$$

which reduces to appropriate limits S_s^{LW} and S_c^{LW} for $R \to 1$ and $D \to \infty$, respectively. The role of polar interactions can thus be conveniently illustrated for a substrate considered to be homogeneous in its LW properties, *viz.*, $R \to 1$ or $D \to \infty$. This is taken up first, followed by the nonlinear influences of the LW nonhomogeneity of the coated substrate.

Homogeneous Substrate ($R \to 1$ or $D \to \infty$): Role of Polar Interactions. The film instability (eqs 27 and 28) is governed by two equilibrium macroscopic parameters of wetting $-S_k^{LW}$ and S_k^P, where k refers to the substrate or coating for $R = 1$ or $D \to \infty$, respectively. For completely apolar ($S_k^P = 0$) or completely polar ($S_k^{LW} = 0$) films, the length scale of the instability (and the time of breakup) may be related to the equilibrium contact angle, θ, with the help of eq 2, *viz.*

$$\lambda_{ML} = \left(\frac{2\pi h_0^2}{3d_0}\right)(1 - \cos\theta)^{-1/2} \quad (33a)$$

$$\lambda_{ML}^* = 2\sqrt{2}\pi l_0(1 - \cos\theta)^{-1/2} \exp\left[\frac{d_0 - h_0}{2l_0}\right] \quad (33b)$$

Clearly, decreased wettability (increased θ) engenders stronger film instability with a greater density of holes, shorter λ_{ML}, and faster film breakup (*e.g.*, eq 28).

Based on *linear theory*, parts a and b of Figure 3 show the variations of the time of rupture for water films on a variety of apolar ($S^P = -102$ mJ/m^2) and polar (variable S^P) substrates, respectively. Lifetimes of relatively thin films (<8 nm) are governed entirely by the strength of short-ranged polar interactions (S^P), regardless of S^{LW}. However, the rupture of thicker films (>12 nm) is controlled solely by the magnitude of S^{LW}, and the polarity (S^P) of the substrate or fluid makes little difference. For completely polar systems, a rapid breakup ($t_{ML} < 1$ s) of aqueous films is possible only when the local thickness becomes smaller than about 10 nm. However, even a small (residual) apolar component of the spreading pressure can engender fast

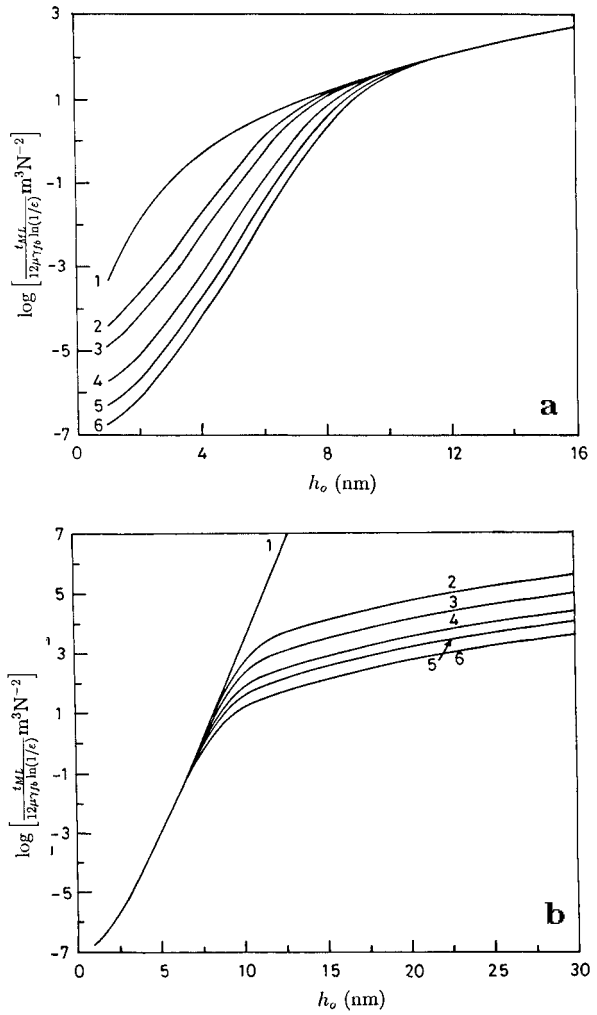

Figure 3. Influence of film thickness and the apolar and polar components of spreading coefficient on the normalized time of film breakup from the linear theory: (a) $S^P = -102$ mJ/m^2; curves 1−6 correspond to S^{LW} (in mJ/m^2) values of 0, −1, −2, −4, −6, and −10, respectively. (b) $S^{LW} = -6$ mJ/m^2, curves 1−6 correspond to (S^P, θ) values of (0, 23), (−5, 32), (−10, 39), (−30, 60), (−60, 85), and (−102, 119), respectively (S^P in mJ/m^2, θ in degrees).

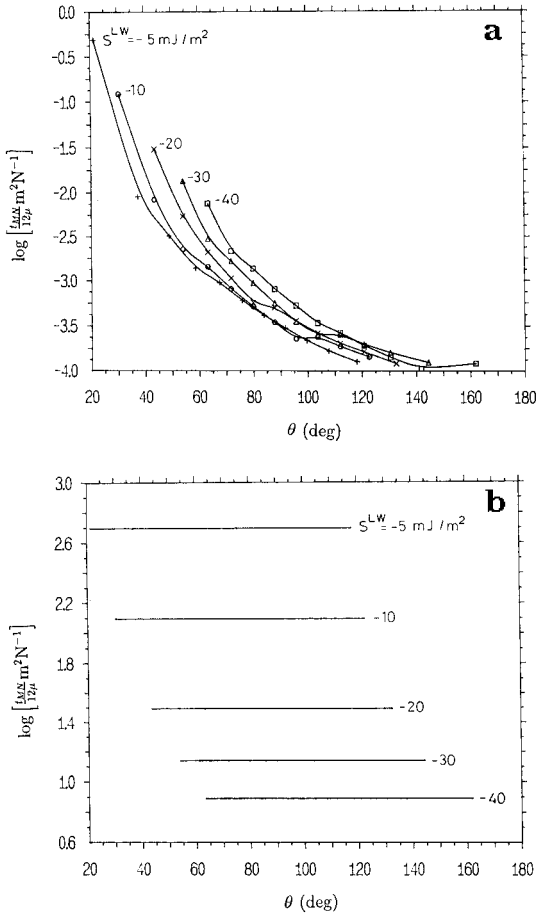

Figure 4. Variation of the breakup time with the equilibrium contact angle (or S^P) and S^{LW}: (a) 5 nm thick film ($\epsilon = 0.01$, $\gamma_{fb} = 72.8$ mJ/m^2); (b) same as a but for a 20 nm thick film.

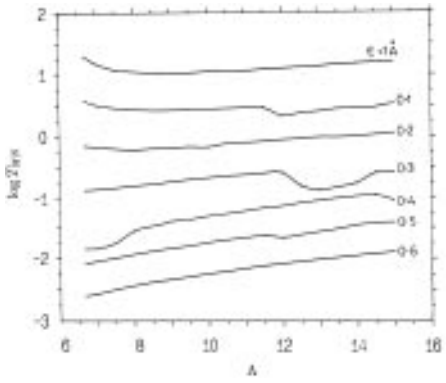

Figure 5. Nonlinear mode selection for $S^{LW} = -17.2$, $S^P = -60$ (in mJ/m^2), $h_0 = 10$ nm, and $\Lambda_{ML} = 8.7$.

breakup of thicker films (curves 2−6 of Figure 3a). While the stability of thin and thick films is governed by S^P and S^{LW}, respectively, the equilibrium wettability (contact angle) is equally affected by both S^{LW} and S^P (eq 2). Thus, the film stability cannot, in general, be correlated only to the equilibrium wettability (θ).

The above qualitative conclusions based on the linear instability are entirely supported by numerical solutions of the nonlinear equation (20) with ($R = 1$). Parts a and b of Figure 4 display lifetimes t_{MN} evaluated from the nonlinear theory for relatively thin and thick films, respectively. In these figures, the variation of the contact angle is due to the variation of S^P, since S^{LW} has a fixed value for each curve. As announced earlier, the breakup time of thick films (Figure 4b) depends only on S^{LW}, regardless of the equilibrium wettability (θ or S^P). For thinner films, contact angle (or S^P) has a more profound influence, compared to the influence of S^{LW}. However, in contrast to the predictions of the linear theory (Figure 3a), the influence of S^{LW} on the breakup time of thin films is not insignificant (*e.g.*, 5 nm thick film of Figure 4a).

The most unstable mode of the nonlinear theory, Λ_{MN}, can be isolated by solving eq 20 for many different values of $\Lambda > \Lambda_C$ in the neighborhood of Λ_{ML}. The dependence of the breakup time on the wavelength is shown in Figure 5 for different initial amplitudes. The minimum time of rupture is usually obtained in the vicinity of the dominant linear wave ($\Lambda_{ML} \approx 8.7$) for small initial amplitudes, but it shifts closer to the Λ_C for increasingly large amplitudes. There is also the possibility of the subcritical ($\Lambda < \Lambda_C$) waves of the linear theory becoming dominant for large amplitudes ($\epsilon > 0.3$ in Figure 5). The most interesting nonlinear aspect apparent from Figure 5 is that the minima are rather flat and broad, which implies that waves of many different wavelengths can be considered to be dominant, in that they can engender breakup on very similar time scales. As is shown later in Figure 9, the same conclusion also holds for the dominant length scale of instability on coated substrates. A large random scatter in the

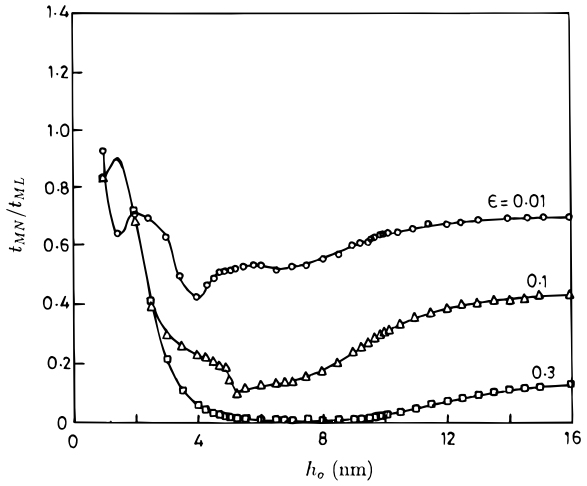

Figure 6. Comparison between the nonlinear and linear theories [$S^{LW} = -17.2$, $S^P = -60$ (in mJ/m^2)]. Markers represent simulations; lines are only to guide the eye.

interhole spacing (from its mean value) is indeed witnessed in experiments on the breakup of thin polymeric films.[30,32] Insensitivity of breakup times on the length scale is one of the reasons for this observation, but other nonlinear factors (*e.g.*, hole−hole interaction in 3D) are also involved.

Figure 6 shows the ratio of the minimum times of rupture as calculated from the nonlinear and linear theories. Asymptotic values of the ratio for thick films (>15 nm) are characteristic of completely apolar systems, as the rate-determining step for rupture is the initial slow growth of disturbances, which is governed largely by the LW interactions for thick films. Nonlinearities associated with the apolar and polar interactions conspire to produce explosive rupture of films for intermediate thicknesses (3−10 nm), where the linear theory may overestimate the time of rupture by several orders of magnitude, especially for relatively large ϵ.

Finally parts a and b of Figure 7 depict the nonlinear process of film breakup and formation of holes, starting with a small random disturbance ($\epsilon = 0.01$) and a large periodic disturbance ($\epsilon = 0.3$), respectively. For the simulation of Figure 7a, Λ was chosen to be $2\Lambda_{ML}$. Clearly, the length scale of the instability is accurately predicted by the linear theory, since a two-hole structure is indeed visible in Figure 7a. In contrast to the symmetric waves predicted by the linear theory (eq 23), the actual hole/film profile is markedly asymmetric. Regions of the film away from the developing hole remain largely undisturbed, especially during the last explosive (nonlinear) phase of the growth. It may be noted that the (nondimensional) *x*-scale in Figure 7 is greatly compressed. The actual (dimensional) *x*-scale is several orders of magnitude larger than the film thickness, so that slopes are indeed small, and the visual appearance of the film away from the hole should be largely uniform.

For the large initial disturbance (Figure 7b), a rudimentary rim appears around the hole. After the film breakup, the hole (dry spot) grows further on the substrate,[30] resulting in the formation (for small ϵ) or growth (for large ϵ) of the rim. However, eq 20 breaks down after the appearance of a true three-phase contact line and therefore cannot be used to track the further evolution of the hole/rim. The removal of singularity in eq 20 as $H \rightarrow 0$ and analysis of hole growth after the film breakup require substantial modifications of the

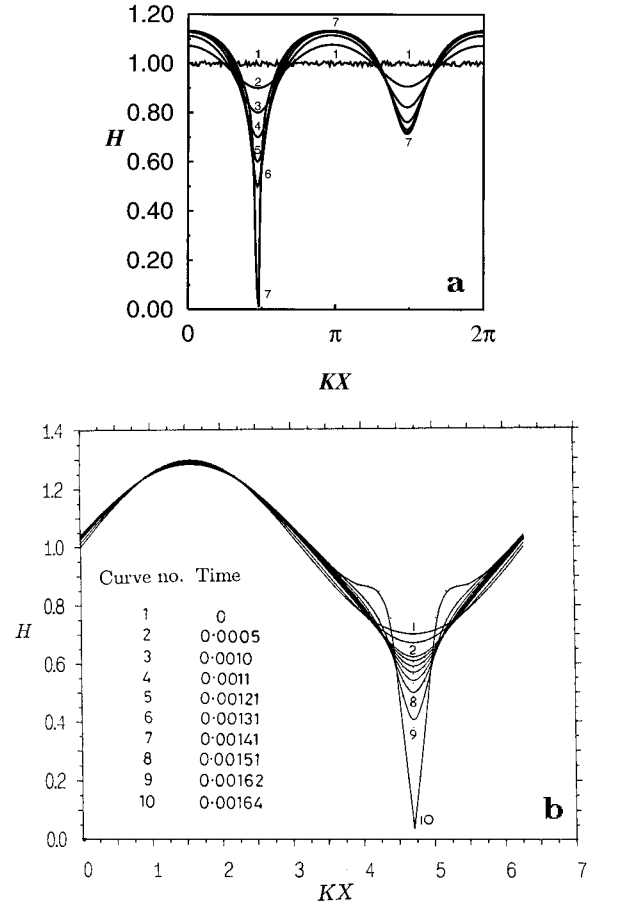

Figure 7. Evolution of the film instability [$S^{LW} = -17.2$, $S^P = -60$ (in mJ/m^2), $h_0 = 5$ nm, $\Lambda_{ML} = 2.4$]: (a) Evolution starting with a small ($\epsilon = 0.01$) random disturbance with $\Lambda = 2\Lambda_{ML}$. Curves 1−7 correspond to T ($\times 10^4$) = 0, 922, 1002, 1023, 1029, 1031, and 1032, respectively. (b) Evolution starting with a large ($\epsilon = 0.3$) periodic disturbance with $\Lambda = \Lambda_{ML}$.

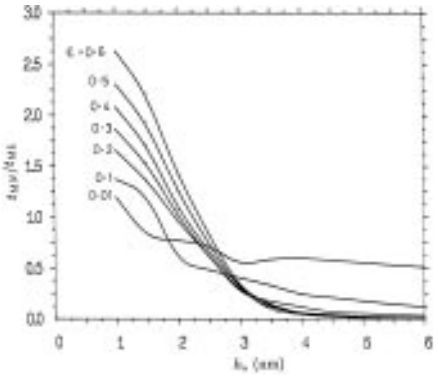

Figure 8. Comparison of breakup times as calculated from the nonlinear and linear theories for completely polar films ($S^{LW} = 0$).

theory and numerical methods (Fourier collocation also breaks down). This work is currently being pursued and will be published elsewhere.

Nonlinear Effects in Completely Polar Films. While the nonlinear stability of completely apolar films on uncoated substrates has been studied extensively,[7,12,22,28,38,43,44,48,56,57] comparable results for completely polar systems are not available. The linear results are given by eqs 24−31 and 33b, and the nonlinear effects are governed by eq 22.

Figure 8 shows the ratio of lifetimes as calculated from the nonlinear and linear theories. The linear theory underestimates the breakup time, *i.e.*, t_{MN}/t_{ML}

> 1 below some thickness in the range of 1.5−2.5 nm, depending on the amplitude. A qualitative explanation is as follows. The ratio of destabilizing terms from the nonlinear and linear theories is

$$R_d = H^3 \exp[(d - H)/l]/\exp[(d - 1)/l] \qquad (34)$$

The maximum value of R_d occurs at $H = 3l$ or $h = 3l_0$. It is easily verified that $R_d < 1$ for $h_0 > 3l_0$, whereas $R_d > 1$ for $h_0 < 3l_0$. In other words, if the minimum initial thickness ($h_0 - \epsilon$) is less than about $3l_0$ ($l_0 = 0.6$ nm in simulations), t_{MN}/t_{ML} should become greater than 1, which is the case in Figure 8. More interestingly, the actual (nonlinear) breakup time may be up to several orders of magnitude smaller than the linear theory predictions for thicker films (>4 nm) subjected to large perturbations.

In summary, while the equilibrium wettability (macroscopic contact angle) is determined by S^{LW} and S^P, the stability and lifetimes of thin and thick films are governed by the strengths of the polar (S^P) and apolar (S^{LW}) interactions, respectively. Thus, if the wettability of a substrate is increased by a coating with LW properties similar to that of the substrate, it would be ineffective in altering the initial stages of instability and dewetting (film rupture) of relatively thick films. This conclusion partially explains the behavior of thick (>10 nm) polymer films on silicon substrates modified by coatings of different equilibrium wettability.[30,32] The initial stages of the instability and dewetting were indeed found to be rather unaffected by the surface properties of the coating. The explanation given so far for this observation is, however, incomplete, in that the coatings used in the experiments may have also differed in their LW properties (S^{LW}). The effect of LW properties of the substrate and coating on the film stability is now considered.

Coated Substrate: Role of Apolor Interactions ($S^P = 0$). The linear stability results of uncoated and coated substrates become identical by defining an effective LW component of the spreading coefficient (eq 32). Thus, results of linear stability analysis displayed in Figure 3a,b are also valid coated substrates if S_s^{LW} is interpreted as S_e^{LW}. Whether S_e^{LW} is closer to S_s^{LW} or S_c^{LW} *depends on the thickness of the coating relative to the initial mean thickness of the film; i.e.,* $S_e^{LW} \rightarrow S_s^{LW}$ for D ($=\delta/h_0$) $\rightarrow 0$, and $S_e^{LW} \rightarrow S_c^{LW}$ for $D \rightarrow \infty$. Stability of relatively thick films is therefore governed largely by the substrate LW properties, regardless of the surface properties of thin (usually nanometer-sized) coating. In contrast to the film stability, however, the equilibrium wettability (contact angle) is governed solely, or largely, by properties of the coating (eq 17). Thus, the effect of coating on the film instability is completely screened for very thick ($D \ll 1$, $RD \ll 1$) films; *i.e.*, neither the apolar (S_c^{LW}) and polar (S_c^P) components of the spreading coefficient for the coating nor the wettability (θ_c) of the coated substrate should have much influence on the film breakup.

The sensitivity of length and time scales of the instability to the coating properties can be examined by the linear theory. The ratio (R_λ) of the dominant wavelengths with and without the coating is given by (from eq 27).

$$R_\lambda = [(1 + D)^{-4}(1 - R) + R]^{-1/2} = \left[\frac{S_e^{LW}}{S_s^{LW}}\right]^{-1/2} \qquad (35)$$

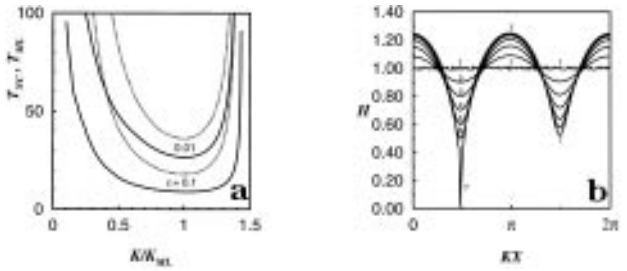

Figure 9. Nonlinear mode selection for coated substrates: (a) Variation of nonlinear rupture time (solid lines, $R = 0.1$, $D = 0.1$). Linear theory results (dashed lines) are also shown for comparison. (b) Evolution and mode selection starting with a small ($\epsilon = 0.01$) random disturbance ($\Lambda = 2\Lambda_{ML} = 11.8$, $R = 5$, $D = 0.1$). Curves 1−7 correspond to T ($\times 10^2$) = 0, 346, 389, 407, 415, 418, and 420, respectively.

In contrast, the ratio (R_T) of times of rupture with and without coating is (from eq 28).

$$R_T = [(1 + D)^{-4}(1 - R) + R]^{-2} = R_\lambda^4 \qquad (36)$$

Thus, while the length scale is only weakly dependent ($R_\lambda \sim 1$) on the coating properties (especially for D and $DR \ll 1$), the time of rupture is rather more sensitive to the coating properties (D and R).

Equation 35 explains a somewhat puzzling aspect of experiments[30,32] on the rupture of thin (<100 nm) polystyrene (PS) films. The number density of holes was found[41] to be rather insensitive to the nature (wettability) of different nanosized coatings applied to silicon wafers (substrate). The equilibrium contact angle of PS ranged from 22° to 48° on different coatings.[32] This gives S_c^{LW} for PS in the range of −2.8 to −12.5 mJ/m^2 (based on eq 17 after neglect[41] of polar interactions for PS and $\gamma_{fb} = 38$ mJ/m^2) and R in the range of 0.135−1.5 (since $S_s^{LW} = -8.1$ mJ/m^2 for PS on silicon substrate[41]). In the same experiments, D ($=\delta/h_0$) was in the range of 0.01−0.1. Under these conditions, eq 35 indeed predicts $R_\lambda \sim 1$ to a very good approximation (the maximum deviation for R_λ is about 10% at $D = 0.1$ and even less for smaller D). The kinetics of rupture is, however, much more sensitive to the coating, as R_T varies between 0.74 and 1.6 under the same conditions ($D = 0.1$, $R \sim 0.35$−1.5).

The relative importance of the nonlinear LW interactions with the coating and substrate can be quantified by numerical solution of eq 20 with $S_c^P = 0$. Figure 9a addresses the problem of nonlinear mode selection. The dominant nonlinear mode has a wavenumber slightly below K_{ML}. The minimum in the time of rupture is, however, rather flat, which obviates the need for repeated solution of eq 20 for different wavenumbers, in order to isolate the most unstable wave. The mean length scale of the instability can therefore be accurately predicted by the linear theory, at least for small initial amplitudes ($\epsilon < 0.1$). Figure 9b shows the typical evolution of the film profile until rupture, starting with a small ($\epsilon = 0.01$) random disturbance ($\Lambda = 2\Lambda_{ML}$). All of the above qualitative features are similar to Figure 7a discussed earlier. The simulation also confirms the expectation of the linear theory for the dominant wavelength.

Parts a and b of Figure 10 illustrate the influence of coating on the breakup time, compared to the case of the pure substrate. The ratio (T_{NC}/T_{NS}) of nonlinear breakup times on coated and uncoated substrates increases when the coating is more wettable than the

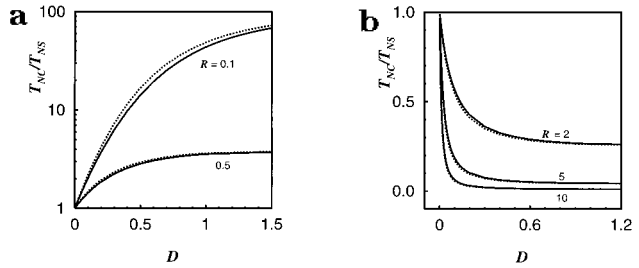

Figure 10. Influence of coating on the film breakup time: (a) Coating is more wettable than the substrate ($R < 1$). (b) Coating is less wettable than the substrate ($R > 1$). Curves for different initial amplitudes, $\epsilon = 0.01$ (solid lines) and 0.1 (dashed lines) virtually coincide.

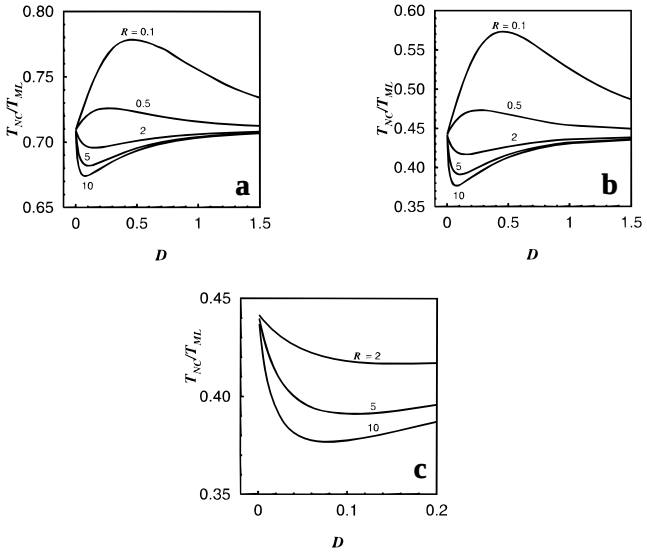

Figure 11. Ratio of breakup times from nonlinear and linear theories, respectively: (a) $\epsilon = 0.01$; (b) $\epsilon = 0.1$; (c) magnified view of the region, $D < 0.2$, $R > 1$, in b.

substrate ($R < 1$, since $|S_c^{LW}| < |S_s^{LW}|$). The effect of underlying substrate on the breakup time, however, remains significant even for coatings as thick as the film (Figure 10a), especially for more wettable coatings ($R < 1$). This is because, for more wettable coatings, the film breakup is increasingly controlled by the wettability (S_s^{LW}) of the substrate.

When the coating is less wettable than the substrate ($|S_c^{LW}| < |S_s^{LW}|$), the breakup time on the coated substrate declines rapidly and reaches a value characteristic of the pure coating material, *even for coatings as thin as about one-tenth the size of the film* (Figure 10b). Interestingly, conclusions arrived at in Figure 10a,b are independent of the initial amplitude of disturbances, as results shown in these figures turned out to be virtually identical for $\epsilon = 0.01$ and 0.1 except when R is very small (<0.1). This observation implies that effects of nonlinearities on the breakup time are very similar for both coated and uncoated substrates. Thus, R_T from eq 36 is a very good approximation for the nonlinear results displayed in Figure 10a,b. In particular, the asymptotic values of (T_{NC}/T_{NS}) should equal R^{-2}, which is indeed seen to be the case in computations.

Finally, parts a ($\epsilon = 0.01$) and b ($\epsilon = 0.1$) of Figure 11 quantify the effect of nonlinearities on the breakup time of films on coated substrates. The discrepancy between the nonlinear and linear theories increases with increased amplitude, as is clear from a comparison of parts a and b of Figure 11. The discrepancy also increases as the coating becomes increasingly less wettable, *i.e.*, as R increases. The limiting values of the ratio (T_{NC}/T_{ML}) for uncoated substrate ($\delta = 0$), as well as for thick coatings ($D \rightarrow \infty$), are identical to the value obtained for an uncoated substrate.[38,56,57] The minima of T_{NC}/T_{ML} for $R > 1$ can be explained as follows. In the linear approximation, the breakup time on a very thin (small δ/h_0) coating is governed essentially by the substrate, regardless of the coating properties. In reality, the influence of the coating is felt during the later stages of the growth of instability, once the local film thickness declines sufficiently. If the coating is less wettable ($R > 1$), the effect of coating accelerates the film breakup compared to the linear theory predictions. Further, the nonlinear destabilization brought about by the coating increases as the coating thickness increases from zero. Thus, for sufficiently thin coatings, T_{NC}/T_{ML} declines with the coating thickness. A better view of this region is provided in Figure 11c. The ratio T_{NC}/T_{ML} cannot, however, decline indefinitely with D since, for $\delta \rightarrow \infty$, it must reach a value characteristic of the uncoated (pure) substrate, *viz.*, the value of T_{NC}/T_{ML} at $\delta = 0$. Similarly, when the coating is more wettable than the substrate ($R < 1$), an inverse reasoning helps clarify the basis of the maxima witnessed in Figure 11a,b.

In summary, we have theoretically studied the linear and nonlinear stability and lifetimes of thin polar and apolar fluid films on coated and uncoated nonwettable substrates. The attention has been confined to films which are subject to purely attractive (destabilizing) long- and short-range intermolecular force. The stability, lifetimes, and contact angles are related to apolar and polar components of the spreading coefficient. A methodology is also presented for determination of these equilibrium macroscopic parameters of wetting from facile measurements of contact angles. In this way, the *dynamic behavior of nonequilibrium microscopic films* can be correlated to the *equilibrium macroscopic parameters of wetting* which characterize the coating and the substrate. This should be helpful for the design and interpretation of future experiments involving thin films on coated substrates.

Acknowledgment

Authors have greatly benefited from discussions with Günter Reiter, who also brought the problem of stability of thin films on coated substrates to our attention.

Appendix

S_k^{LW} and S_k^P for water ($\gamma_f^{LW} = 21.8$, $\gamma_f^P = 51$; in mJ/m^2) or other polar liquids on any smooth, homogeneous surface (k) can be determined by the following measurements of the equilibrium contact angles. First, the contact angle of an apolar "probe" liquid (p) of known surface tension is recorded. The Young equation (eq 2) with $S^P = 0$ then gives S^{LW} for the probe liquid on the surface. Since $\gamma_p^{LW} = \gamma_p$ (for the apolar probe liquid) is known and $\gamma_b^{LW} = 0$ (for air), eq 10 with f = p gives the LW component of the surface tension of (γ_k^{LW}) for the substrate being probed. Now, S_k^{LW} of water ($\gamma_f^{LW} = 21.8$ mJ/m^2) on the same surface is easily estimated from eq 10 if the LW component of surface tension of the bounding fluid is also known. γ^{LW} for many liquids are known or can be estimated. For apolar bounding media, γ_b^{LW} also equals the total surface tension, which is easily determined by a variety of techniques.

Having found S_k^{LW} for the system under investigation (1−3−2), S^P can be obtained from the Young equation,

$$\cos\theta = 1 + \frac{S_k^{LW} + S_k^P}{\gamma_{fb}} \qquad (A.1)$$

by measuring the contact angle (θ) of liquid (f) on the substrate (k) in the presence of bounding fluid (b). γ_{fb} in eq A.1 can be directly measured or estimated either from eqs 9 and 13 or from the theory of acid−base interactions. If b is a gas, γ_{fb} equals the total surface tension of fluid f (for water, $\gamma_f = 72.8$ mJ/m^2). If b is an apolar liquid, $\gamma_{fb} = \gamma_{fb}^{LW} + \gamma_{fb}^{P}$ where γ_f^P for water is 51 mJ/m^2 and γ_{fb}^{LW} is evaluated from eq 9.

It is also of interest to note that if bounding liquid is apolar, the definition of S_k^P (eq 12) simplifies to

$$S_k^P = \gamma_k^P - \gamma_f^P - \gamma_{kf}^P \qquad (A.2)$$

In such an event, the same value of S_k^P is obtained regardless of whether bounding fluid is a condensed medium or gas. The apolar properties of the bounding fluid only affect S_k^{LW}. For this particular case, S_k^P for the system (k−f−b) can also be obtained by measuring the contact angle (θ) of f on k in the absence of b and writing the Young equation for the system (k−f−air) as

$$\cos\theta = 1 + \frac{(S_k^{LW} + S_k^P)}{\gamma_f} \qquad (A.3)$$

However, in contrast to eq A.1, S_k^{LW} in eq A.3 is for the system k−f−air, *i.e.*, $S^{LW} = 2\sqrt{\gamma_k^{LW}}(\sqrt{\gamma_k^{LW}} - \sqrt{\gamma_f^{LW}})$ from eq 10.

It may be noted that, in the above method, a "model" of polar interactions is not assumed in order to evaluate S_k^P.

Literature Cited

(1) Brochard-Wyart, F.; di Meglio, J. M.; Quere, D.; de Gennes, P. G. Spreading of non-volatile liquids in a continuum picture. *Langmuir* **1991**, *7*, 335.

(2) Brochard-Wyart, F.; de Gennes, P. G.; Hervet, H. Wetting of stratified solids. *Adv. Colloid Interface Sci.* **1991**, *34*, 561.

(3) Burelbach, J. P.; Bankoff, S. G.; Davis, S. H. Nonlinear stability of evaporating/condensing liquid films. *J. Fluid Mech.* **1988**, *195*, 463.

(4) Chauraev, N. V. Wetting films and wetting. *Rev. Phys. Appl.* **1988**, *23*, 975.

(5) de Gennes, P. G. Wetting: Statics and Dynamics. *Rev. Mod. Phys.* **1985**, *57*, 827.

(6) De Coninck, J.; Fraysse, N.; Valignant, M. P.; Cazabat, A. M. A microscopic simulation of the spreading of layered droplets. *Langmuir* **1993**, *9*, 1906.

(7) De Wit, A.; Gallez, D.; Christov, C. I. Nonlinear evolution equation for thin liquid films with insoluble surfactants. *Phys. Fluids* **1994**, *6*, 3256.

(8) Derjaguin, B. V. The definition and magnitude of disjoining pressure and its role in the statics and dynamics of thin liquid films. *Kolloid. Zh.* **1955**, *17*, 205.

(9) Dimitrov, D. S. Dynamic interactions between approaching surfaces of biological interest. *Prog. Surf. Sci.* **1983**, *14*, 295.

(10) Extrand, C. Continuity of very thin polymer films. *Langmuir* **1993**, *9*, 475.

(11) Forcada, M. L.; Mate, C. M. Molecular Layering during evaporation of ultrathin liquid films. *Nature* **1993**, *363*, 527.

(12) Gallez, D. Nonlinear stability analysis for animal cell adhesion to solid support. *Colloids Surf. B* **1994**, *2*, 273.

(13) Gallez, D.; Coakley, W. T. Interfacial instability at cell membranes. *Prog. Biophys. Mol. Biol.* **1986**, *48*, 155.

(14) Guerra, J. M.; Srinivasrao, M.; Stein, R. S. Photon tunneling microscopy of polymeric surfaces. *Science* **1992**, *68*, 75.

(15) Gupta, A.; Sharma, M. M. Stability of thin aqueous films on solid surfaces. *J. Colloid Interface Sci.* **1992**, *149*, 392.

(16) Hamaker, H. C. The London−van der Waals attraction between spherical particles. *Physica* **1937**, *4*, 1058.

(17) Hirasaki, G. J. Thermodynamics of thin films and three phase contact regions. In *Interfacial Phenomena in Petroleum Recovery*; Morrow, N. R., ed.; Marcell Dekker Inc.: New York, 1991; Chapter 2, pp 23−27.

(18) Israelachvili, J. N. *Intermolecular and Surface Forces*; Academic Press: London, 1985.

(19) Jameel, A. T.; Sharma, A. Morphological phase separation in thin liquid films: Equilibrium contact angles of nanodrops coexisting with thin films. *J. Colloid Interface Sci.* **1994**, *164*, 416.

(20) Janczuk, B.; Chibowski, E. Interpretation of contact angles in solid−hydrocarbon−water system. *J. Colloid Interface Sci.* **1983**, *95*, 268.

(21) Kaelble, D. H. Dispersion-polar surface tension properties of organic solids. *J. Adhes.* **1970**, *2*, 66.

(22) Khesgi, H. S.; Scriven, L. E. Dewetting: Nucleation and growth of dry regions. *Chem. Eng. Sci.* **1991**, *46*, 519.

(23) Ko, Y. C.; Ratner, B. D.; Hoffman, A. S. Characterization of hydrophilic−hydrophobic polymeric surfaces by contact angle measurements. *J. Colloid Interface Sci.* **1981**, *82*, 25.

(24) Langmuir, I. *Trans. Faraday Soc.* **1920**, *15*, 62.

(25) Leger, L.; Joanny, J. F. Liquid spreading. *Rep. Prog. Phys.* **1992**, *55*, 431.

(26) Leibler, L.; Ajdari, A.; Mourran, A.; Coulon, G.; Chatenay, D. Wetting of grafted polymer surfaces by compatible chains. In *Ordering in Molecular Systems*; Teramato, A., Kobayashi, M., Norisuje, T., Eds.; Springer-Verlag: Berlin, 1994.

(27) Malderelli, C.; Jain, R. K.; Ivanov, I. B.; Ruckenstein, E. Stability of symmetric and unsymmetric thin liquid films to short and long wavelength perturbations. *J. Colloid Interface Sci.* **1980**, *78*, 118.

(28) Mitlin, V. S. Dewetting of solid surfaces: Anology to spinodal decomposition. *J. Colloid Interface Sci.* **1993**, *156*, 491.

(29) Nir, S.; Vassilieff, C. S. van der Waals interactions. In *Thin Liquid Films*; Ivanov, I. B., Ed.; Surfactant Science Series 29; Marcell Dekker: New York, 1988.

(30) Reiter, G. Dewetting of thin polymer films. *Phys. Rev. Lett.* **1992**, *68*, 75.

(31) Reiter, G. Dewetting of polymers in films thinner than their unperturbed size. *Europhys. Lett.* **1993**, *23*, 579.

(32) Reiter, G. Unstable thin polymer films: Rupture and dewetting processes. *Langmuir* **1993**, *9*, 1344.

(33) Reiter, G. Dewetting as a probe of polymer mobility in thin films. *Macromolecules* **1994**, *27*, 3046.

(34) Reiter, G.; Auroy, P.; Auvray, L. Instabilities of thin polymer films on layers of chemically identical grafted molecules. *Macromolecules* **1996**, *29*, 2150.

(35) Ruckenstein, E.; Jain, R. K. Spontaneous rupture of thin liquid films. *J. Chem. Soc., Faraday Trans. II* **1974**, *70*, 132.

(36) Sharma, A. Relationship of thin film stability and morphology to macroscopic parameters of wetting in the apolar and polar systems. *Langmuir* **1993**, *9*, 861.

(37) Sharma, A. Equilibrium contact angles and film thicknesses in the apolar and polar systems. *Langmuir* **1993**, *9*, 3580.

(38) Sharma, A.; Jameel, A. T. Nonlinear stability, rupture and morphological phase separation of thin liquid films on apolar and polar substrates. *J. Colloid Interface Sci.* **1993**, *161*, 190.

(39) Sharma, A.; Jameel, A. T. Stability of thin polar films on non-wettable substrates. *J. Chem. Soc., Faraday Trans.* **1994**, *90*, 625.

(40) Sharma, A.; Kishore, C. S.; Salaniwal, S.; Ruckenstein, E. Nonlinear stability and rupture of ultrathin free films. *Phys. Fluids A* **1995**, *9*, 1832.

(41) Sharma, A.; Reiter, G. Instability of thin polymer films on coated substrates: Rupture, dewetting and drop formation. *J. Colloid Interface Sci.* **1996**, *178*, 383.

(42) Sharma, A.; Ruckenstein, E. The role of lipid abnormalities, aqueous and mucus deficiencies in the tear film breakup and implications for tear substitutes and contact lens tolerance. *J. Colloid Interface Sci.* **1986**, *111*, 8.

(43) Sharma, A.; Ruckenstein, E. An analytical nonlinear theory of thin film rupture and its application to wetting films. *J. Colloid Interface Sci.* **1986**, *113*, 456.

(44) Sharma, A.; Ruckenstein, E. Finite amplitude instability of thin free and wetting films. *Langmuir* **1986**, *2*, 480.

(45) Sharma, A.; Ruckenstein, E. Dynamics and lifetimes of thin evaporating liquid films. *Phys. Chem. Hydrodyn.* **1988**, *10*, 675.

(46) Shull, K. R. Wetting autophobicity of polymer melts. *Faraday Discuss.* **1994**, *98*, 203.

(47) Sheludko, A. Thin liquid films. *Adv. Colloid Interface Sci.* **1967**, *1*, 391.

(48) Teletzke, G. F.; Davis, S. H.; Scriven, L. E. How liquids spread on solids. *Chem. Eng. Commun.* **1987**, *55*, 41.

(49) van Oss, C. J. Surface properties of fibrinogen and fibrin. *J. Protein Chem.* **1990**, *9*, 487.

(50) van Oss, C. J. Acid−base interfacial interactions in aqueous media. *Colloids Surf. A* **1993**, *78*, 1.

(51) van Oss, C. J.; Chaudhury, M. K.; Good, R. J. Interfacial Lifshitz−van der Waals and polar interactions in macroscopic systems. *Chem. Rev.* **1988**, *88*, 927.

(52) van Oss, C. J.; Chaudhury, M. K.; Good, R. J. The mechanism of phase separation of polymers in organic media−apolar and polar systems. *Sep. Sci. Technol.* **1989**, *24*, 15.

(53) van Oss, C. J.; Good, R. J.; Chaudhury, M. K. Additive and nonadditive surface tension components and interpretation of contact angles. *Langmuir* **1988**, *4*, 884.

(54) Vrij, A. Possible mechanisms for the spontaneous rupture of thin free liquid films. *Discuss. Faraday Soc.* **1966**, *42*, 23.

(55) Wicks, Z. W.; Jones, F. N.; Pappas, S. P. *Organic coatings: Science and Technology*; Wiley: New York, 1992.

(56) Williams, M. B.; Davis, S. H. Nonlinear theory of film rupture. *J. Colloid Interface Sci.* **1982**, *90*, 220.

(57) Yiantsios, S. G.; Higgins, B. G. Rupture of thin films: Nonlinear stability analysis. *J. Colloid Interface Sci.* **1991**, *147*, 341.

(58) Zhao, W.; Rafailovich, M. H.; Sokolov, J.; Fetters, L. J.; Plano, R.; et al. Wetting properties of thin liquid polyethylene propylene films. *Phys. Rev. Lett.* **1993**, *70*, 1453.

(59) Zisman, W. A. Relation of equilibrium contact angle to liquid and solid constitution. *Adv. Chem. Soc.* **1964**, *43*, 1.

Received for review December 27, 1995
Accepted April 3, 1996[⊗]

IE950775U

[⊗] Abstract published in *Advance ACS Abstracts,* August 15, 1996.